Supersonic Three-Dimensional Oscillatory Piecewise Continuous Kernel Function Method

E. Nissim* and I. Lottati†
Technion—Israel Institute of Technology, Haifa, Israel

The three-dimensional subsonic piecewise continuous kernel function method formulated for studying oscillatory or steady flows is extended in the present work to planar supersonic wings. The work treats problems associated with the allocation of boxes on the wing, the choice of pressure polynomials, the determination of the collocation points, and the numerical integration techniques resulting from the special form of the supersonic kernel function. Results are presented which confirm the accuracy of the method and its rapid convergence characteristics.

Introduction

SEVERAL numerical methods exist for the computation of oscillatory aerodynamic forces acting on thin wings at supersonic flow. The most widely used is the Mach box method,[1-3] which has some well-known computational problems such as those associated with the convergence of the solution with increasing number of boxes, and the treatment of the "jagged" leading and trailing edges as represented by the Mach boxes. The velocity potential-collocation methods[4,5] eliminate the diaphragm region ahead of subsonic leading edges, but it appears that substantial computational labor is involved and that some computational problems remain which affect the level of accuracy of the results. A numerical procedure had recently been presented[6] which is based on the extension of Evvard's supersonic wing theory[7] to oscillatory flow. However, results relating to the computational efficiency of the method and to the level of accuracy of the computed oscillatory loads (instead of some integrated fractional downwash error) need be published before a full assessment of this method can be made.

The use of the kernel function method (KFM) requires the user to represent the pressure distribution over the wing in terms of pressure functions. It requires therefore a full knowledge of all pressure discontinuities existing over the lifting surface and along their boundaries;[8] in other words, a good knowledge of the characteristics of the unknown solution must be known.[9] In addition, the accuracy and convergence of the results depend on the location of the collocation points over the wing and on whether the integration techniques take full account of the various singularities of the pressure and of the kernel. For these reasons, the use of the KFM is often considered as cumbersome and lacking in generality. However, the results of those kernel function applications which permit taking full account of the above-mentioned points are characterized by a high level of accuracy and rapid convergence.

The formulation of the piecewise continuous kernel function method[10-14] (PCKFM) for subsonic flows was intended to overcome most of the above mentioned problems associated with the KFM. It is shown in Refs. 10-14 that the subsonic PCKFM has the ability to treat pressure discontinuities in a manner similar to the subsonic doublet-lattice method,[15,16] with the added accuracy and rapid convergence characteristics typical of a well formulated kernel function application.

Received March 11, 1982; revision received Dec. 3, 1982.

*Professor, Department of Aeronautical Engineering, Member AIAA.

†Lecturer, Department of Aeronautical Engineering.

In the present work, the extension of the PCKFM to supersonic flows is described. Numerical examples are presented and results are compared with those obtained using exact methods available for wing configurations in steady and in some cases of oscillatory flows.

Description of the Supersonic PCKFM Box-Allocation

The PCKFM can successfully cope with unknown pressure singularities provided their location is known. The wing surface is therefore divided into boxes in such a way that pressure singularities are permitted to lie only along the boundaries of the boxes. Unlike the doublet-lattice method, the boxes used by the PCKFM can be as large as possible provided they exclude pressure discontinuities (implying also discontinuities in the derivatives of the the pressure) from lying within the regions defined by the boundaries of the boxes. The pressure distribution in each box is then represented by a set of continuous polynomials spanning the regions between adjoining singularities. In order to accelerate convergence, pressure singularities are assumed to be known only along the boundaries of the wing; or more specifically, the form of the leading-edge (LE), trailing-edge (TE), and wing-tip pressure singularities are assumed to be known and are treated in the analysis. All other pressure singularities are ignored during the analysis and their consideration is limited to the determination of the boundaries between the different boxes. Examples of such ignored pressure singularities are those arising from geometrical discontinuities such as control surface rotation, LE extensions and break points. The ignored pressure discontinuities are located either on the control surface LE or along the Mach lines which bound conical flow regions and which emanate from points of geometrical discontinuities. It should be pointed out that traditional KFM requires a prior definition of all singularities over the planform of the wing (Ref. 9) before attempting the solution of the problem (thus ensuring good accuracy of results). Figure 1 is an example of a delta wing with subsonic LE. Here the entire wing is represented by a single box. The only pressure singularity lies along the LE (subsonic-LE-type singularity). Since this singularity lies along the boundary of the wing, it is considered in the analysis. Figure 2 shows an example of a clipped delta wing with supersonic LE. Here the entire wing is represented by three boxes and only the wing tip singularity is considered. Figure 3 shows the box allocation on a clipped delta wing with supersonic LE and a TE control surface which spans the whole wing. Here the wing is divided into five boxes. The only pressure singularity considered in the analysis is the wing tip singularity in box 5. All other singularities fall within the category of ignored singularities, since they lie along the boundaries of the boxes and not along the boundaries of the wing.

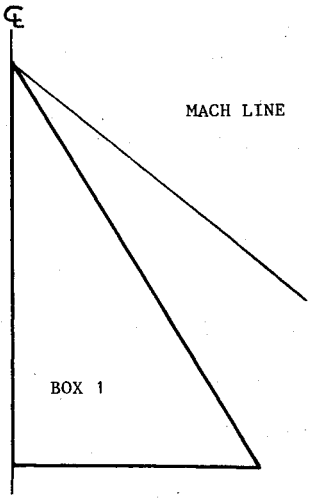

Fig. 1 Single box, subsonic LE, delta wing.

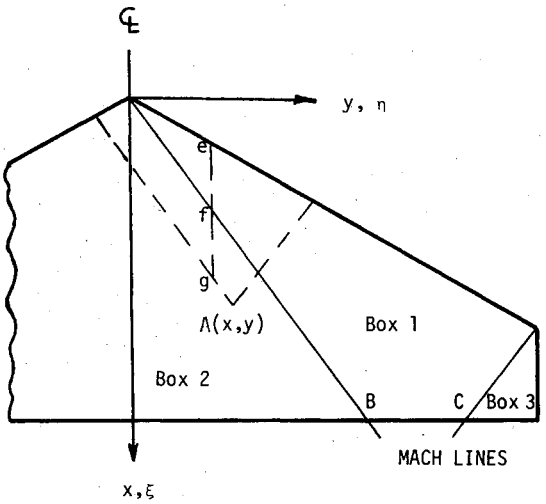

Fig. 2 Box allocation on a supersonic LE, clipped delta wing. Also shown is an example of piecewise integration along segments e-f and f-g.

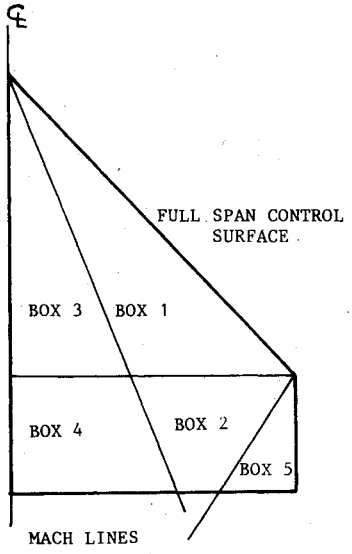

Fig. 3 Box allocation on a supersonic LE clipped delta wing with a full span TE control surface.

Pressure Singularities and Associated Collocation Points

The pressure distribution in each of the boxes formed by the PCKFM is represented in general terms by the following expression:

$$\Delta p(\xi,\eta)/q = \sum_{j=1}^{ns} \sum_{i=1}^{nc} A_m W(\eta) p_j(\eta) w(\xi) p_i(\xi) \qquad (1)$$

where Δp represents the pressure distribution in the box, q the dynamic pressure, A_m a scalar coefficient, ns the number of spanwise polynomials, nc the number of chordwise polynomials, and m is given by $m=(j-1)nc+i$.

The parameters ξ and η represent the coordinates in the chordwise and spanwise directions, respectively. $W(n)$ and $w(\xi)$ represent the assumed singularities in the spanwise and chordwise directions, respectively. If no singularities exist in either one or both directions, $W(\eta)$ or $w(\xi)$ or both are assumed to be equal to 1. $w(\xi)$ is given by the following expressions after transforming ξ into $\bar{\xi}$ so that the box boundaries lie on $\bar{\xi}=\pm 1$.

$$w(\xi) = \frac{1}{\sqrt{1+\bar{\xi}}} \quad \text{for a subsonic LE box}$$

$$= \sqrt{1-\bar{\xi}} \quad \text{for a subsonic TE box}$$

$$= \sqrt{\frac{1-\bar{\xi}}{1+\bar{\xi}}} \quad \text{for a box that includes both LE and TE along its boundaries}$$

$$= 1 \quad \text{for all other boxes, including intermediate boxes}$$

and $p_i(\xi)$ is a polynomial of degree $(i-1)$ which is orthogonal to the singularity represented by $w(\bar{\xi})$ (for more details see Refs. 10-12). $W(\eta)$ can assume either the value of 1 (for any box which does not have the wing tip along its boundary, or the value of $\sqrt{1-\bar{\eta}}$ (relating to boxes on the right wing). The pressure polynomial $p_j(\eta)$ is therefore a polynomial of degree $(j-1)$, which is orthogonal to the singularity represented by $W(\eta)$. Hence, for example, when $W(\eta)=1$, $p_j(\eta)$ represents the Legendre polynomial (see Ref. 17 for more details on orthogonal polynomials).

It can be shown[12] that the overall downwash error is minimized if the collocation points in each box are located at the zeros of the downwash polynomial obtained from the pressure polynomial of one order higher than the highest polynomial used in the box (see also the Appendix of Ref. 12 for a mathematical explanation of this method). The expressions which define the exact locations of these collocation points are presented herein as Appendix. However, it is very important to note that the number of collocation points obtained in the chordwise direction by the aforementioned numerical scheme is greater by one than the degree of the chordwise pressure polynomial employed in Eq. (1) only for the case of an LE box (with either subsonic or supersonic LE). For intermediate and TE boxes, the number of collocation points obtained is greater by two than the degree of the pressure polynomial assumed in the chordwise direction [in Eq. (1)]. This latter case is similar to the subsonic PCKFM, where it had been shown[10,11] that, for accurate definition of the pressure polynomial coefficients, the number of collocation points should correspond to the number of points obtained by the aforementioned numerical scheme and therefore require the introduction of a least square procedure to solve the pressure coefficients. For the spanwise direction, the LE box yields a number of collocation points that is greater by one than the degree of the spanwise pressure

polynomial assumed in Eq. (1) (note that wing tip pressure singularity can never occur in an LE box). For intermediate and TE boxes with wing-tip pressure singularity, the number of spanwise collocation points is greater by two than the degree of the pressure polynomial assumed [in Eq. (1)] in the spanwise direction. For intermediate and TE boxes, without wing-tip pressure singularity, the number of spanwise collocation points is greater by one than the degree of the assumed spanwise pressure polynomial [in Eq. (1)]. It is interesting to note that in the subsonic PCKFM, additional collocation points (i.e., greater by two than the degree of the pressure polynomial used in the analysis) were obtained in the chordwise direction only and never in the spanwise direction. The importance of these additional collocation points and their effect on the accuracy of the results had been demonstrated in Refs. 10 and 11. As a result of this increase in the number of collocation points, a least-square procedure is required for the solution of the unknown pressure polynomial coefficients. This procedure should be performed with great care in supersonic flows for reasons to be explained in later sections of this work.

Numerical Solution for the Pressure Coefficients

The relationship between the pressure distribution over the wing and its resulting downwash is given by

$$w(x,y) = \frac{1}{8\pi} \int \int_s \frac{\Delta p(\xi,\eta)}{q} \frac{K_p(x-\xi, y-\eta, k, M)}{(y-\eta)^2} \, d\xi d\eta \qquad (2)$$

where $w(x,y)$ is the vertical velocity (downwash) at any collocation point (x,y) of the wing; $K_p(x-\xi, y-\eta, k, M)$ the modified kernel function (without the second order pole singularity); k the reduced frequency; M the Mach number; and s the region of integration over the wing.

The kernel function was formulated by Harder and Rodden[18] for steady and oscillatory supersonic flows for the general nonplanar case. However, in the present work, only planar configurations will be considered. The modified kernel function K_p contains an inverse square-root type singularity which can be illustrated by the following simple expression which relates to steady flows

$$K_p(x-\xi, y-\eta, k=0, M) = \frac{-2x_0}{R} \qquad x_0 \geq \beta y_0$$
$$= 0 \qquad x_0 < \beta y_0 \qquad (3)$$

where

$$x_0 = x-\xi; \quad y_0 = y-\eta; \quad \beta = \sqrt{M^2-1}; \quad R = \sqrt{x_0^2 - \beta^2 y_0^2} \qquad (4)$$

It can therefore be seen that the modified kernel has nonzero values only within the forward region on the wing that is bounded by the forward Mach cone emanating from point (x,y). Furthermore, the inverse square-root type singularity of the modified kernel lies along these forward Mach lines as a result of the vanishing of R along these lines. Hence, the region of integration s appearing in Eq. (2) lies ahead of the aforementioned forward Mach lines, with a singularity along these Mach lines. These conclusions hold true also for oscillatory flows. In the following two sections, the problems associated with the integration of Eq. (2) will be treated.

Chordwise Integration of the Kernel-Downwash Expression

For accurate integration in the chordwise direction, the chordwise singularities within the region of integration need be accounted for. This implies that consideration is given to all pressure singularities existing along the boundaries of the wing whereas all pressure singularities over the wing are ignored, in accordance with the assumptions described earlier in this work. However, in addition to the chordwise pressure discontinuities that are considered during the chordwise integration, the chordwise singularity introduced by the supersonic kernel need to be accounted for to ensure the accuracy of the ensuing integration. The expressions for the modified kernel K_p include the term x_0/R for both steady [see Eqs. 3 and 4] and oscillatory flows. Referring to Fig. 4, the region of integration for the collocation point $A(x,y)$ lies between the points ξ_1 and ξ_M. Point ξ_M lies on the forward Mach line emanating from point A. For Gaussian type integration the ξ_1, ξ_M region should be transformed to a region starting at point -1 and ending at point $+1$. Using the following transformation for ξ

$$\xi = \tfrac{1}{2}(\xi_1 + \xi_M) + \tfrac{1}{2}\bar{\xi}(\xi_M - \xi_1)$$

where $\bar{\xi}$ is a new variable which assumes values between -1 and $+1$, the ratio x_0/R assumes the following form

$$\frac{x_0}{R} = \frac{1-\bar{\xi} + \dfrac{2\beta|y-\eta|}{\xi_M - \xi_1}}{(1-\bar{\xi})^{1/2}\left[1-\bar{\xi} + \dfrac{4\beta|y-\eta|}{\xi_M-\xi_1}\right]^{1/2}} \qquad (5)$$

The above expression is very interesting since, for $y-\eta=0$, Eq. (5) yields $x_0/R=1$, implying no singularity at all along the chordwise direction at the collocation chord. It follows, therefore, that if chordwise integration is avoided at $y-\eta=0$, the modified kernel can be assumed to have a chordwise singularity of the type $(1-\bar{\xi})^{-1/2}$. If chordwise integration is performed at $y-\eta=0$, then no chordwise singularity must be assumed to exist in the modified kernel. In addition to the modified kernel singularity, wing boundary pressure singularities must be included in the chordwise integration procedure. For subsonic LE such as in the example shown in Fig. 4, the integration is performed using $(1-\bar{\xi})^{-1/2}(1+\bar{\xi})^{-1/2}$ chordwise singularity or, in other words, a $(1-\bar{\xi}^2)^{-1/2}$ chordwise singularity. Piecewise chordwise integration must at times be performed. One such case is illustrated in Fig. 2 for the collocation point A. The chordwise integration is performed along the segment e-f of box 1, accounting for the LE pressure singularity only. In addition, a separate chordwise integration is performed along the segment f-g of box 2, accounting only for the modified kernel singularity at point g.

Spanwise Integration of the Kernel-Downwash Expression

Following the chordwise integration, the kernel-downwash expression is further integrated in the spanwise direction over the region contained within the wing boundaries and the forward Mach lines emanating from the collocation point. The spanwise integration procedure is identical to the one used in the subsonic PCKFM. The integration region is thus divided into four regions, as indicated in Fig. 4. The integration in region III, where the second order pole lies, is carried out analytically. The integration in regions I, II, and IV takes into account the existence of the second-order pole in region III (using the method suggested in Ref. 19) and the existence of the spanwise pressure singularity (only if necessary). This procedure had been shown[12] to have a large effect on the accuracy of the results, especially when region III is narrowed to small values of the wing fractional span (often dictated by the geometrical singularities).

Solution of the Kernel-Downwash Equations

It has already been shown that the number of collocation points that must be used to ensure adequate accuracy exceeds, in some boxes, the number of unknown pressure coefficients. This requires the use of a least-square procedure in order to

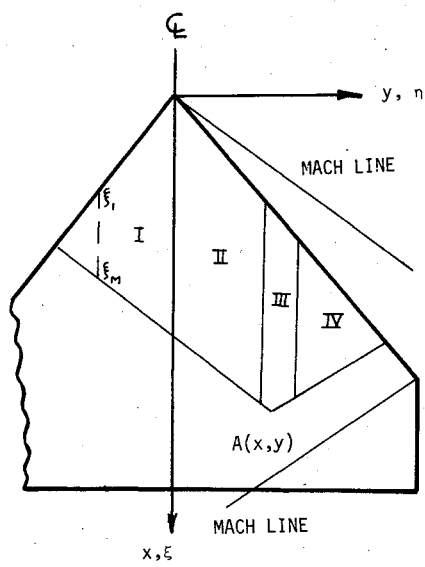

Fig. 4 Regions of integration for the collocation point $A(x,y)$.

solve the kernel-downwash equations. As a result, some unforeseen problems may arise. For illustrative purposes, consider the swept back wing shown in Fig. 2. Following the box allocation procedure described earlier, the wing is divided into three boxes which are separated by the various Mach lines, as shown in Fig. 2. For a general three box example, the kernel-downwash equation has the following form

$$\begin{Bmatrix} w_1 \\ w_2 \\ w_3 \end{Bmatrix} = \begin{bmatrix} B_{11} & B_{12} & B_{13} \\ B_{21} & B_{22} & B_{23} \\ B_{31} & B_{32} & B_{33} \end{bmatrix} \begin{Bmatrix} A_1 \\ A_2 \\ A_3 \end{Bmatrix} \tag{6}$$

where w_i and A_i represent the downwash vector and the vector of pressure polynomial coefficients relating to the ith box, respectively. The matrices B_{ij} are rectangular matrices which might have more rows than columns. For the particular example shown in Fig. 2,

$$B_{12}=B_{13}=B_{23}=B_{32}=0$$

Table 1 Influence of varying the spanwise width of region III on the convergence of the aerodynamic coefficients (delta wing $AR=4$, $M=\sqrt{2}$, $k=0$)[a]

Width of region III	$C_{L\alpha}$	$\epsilon_{L\alpha}$, %	$C_{M\alpha}$	$\epsilon_{M\alpha}$, %	CPU, s
0.02	4.023	0.6	−2.678	0.4	2.59
0.06	3.990	0.3	−2.661	0.2	2.53
0.10	3.962	1.0	−2.638	1.0	2.49

1) Exact values are: $C_{L\alpha}=4$ and $C_{M\alpha}=-2.667$. 2) The integration in region III is performed by the spanwise expansion of the chordwise integrand into a polynomial of the third degree. 3) Three integration points in each of the chordwise subregions. 4) Three spanwise integration points in each of the spanwise subregions. 5) The pressure is described by second-degree polynomials in the spanwise and chordwise directions. 6) The moment is about the wing's apex. 7) Width of region III is 0.02 of the wing semispan. 8) The moment is about the wing LE. 9) Reduced frequency based on root chord (= 10). 10) Reduced frequency based on root chord (= 1).

Table 2 Influence on the aerodynamic coefficients of varying the degree of the spanwise polynomial expansions in region III (delta wing $AR=4$, $M=\sqrt{2}$, $k=0$)[a]

Degree of spanwise polynomial in region III	$C_{L\alpha}$	$\epsilon_{L\alpha}$, %	$C_{M\alpha}$	$\epsilon_{M\alpha}$, %	CPU, s
1	4.022	0.6	−2.676	0.3	2.44
2	4.027	0.7	−2.677	0.4	2.50
3	4.023	0.6	−2.678	0.4	2.59
4	4.031	0.8	−2.667	0.0	2.71

[a] See Table 1, footnotes 1, 3-7.

Table 3 Effect of varying the number of the spanwise and chordwise pressure polynomials on the convergence of the aerodynamic coefficients (delta wing $AR=4$, $M=\sqrt{2}$, $k=0$)[a]

No. of pressure polynomials	$C_{L\alpha}$	$\epsilon_{L\alpha}$, %	$C_{M\alpha}$	$\epsilon_{M\alpha}$, %	CPU,s
	Influence of varying number of spanwise polynomials (number of chordwise pressure polynomials = 3)				
2	4.391	9.8	−2.875	7.8	2.04
3	4.023	0.6	−2.678	0.4	2.59
4	4.034	0.9	−2.679	0.5	3.18
6	3.993	0.2	−2.654	0.5	4.49
	Influence of varying number of chordwise polynomials (number of spanwise pressure polynomials = 3)				
2	4.051	1.3	−2.693	1.0	2.09
3	4.023	0.6	−2.678	0.4	2.59
4	4.030	0.8	−2.685	0.7	3.38
6	4.027	0.7	−2.686	0.7	5.18

[a] See Table 1, footnotes 1-4, 6,7.

This is true since the pressure distribution in box 2 cannot affect the downwash in boxes 1 and 3 (leading to $B_{12}=B_{32}=0$). Similarly, the pressure distribution in box 3 cannot affect the downwash in box 1 and in box 2 (leading to $B_{13}=B_{23}=0$). Hence, the kernel-downwash equation for this example assumes the form

$$\begin{Bmatrix} w_1 \\ w_2 \\ w_3 \end{Bmatrix} = \begin{bmatrix} B_{11} & 0 & 0 \\ B_{21} & B_{22} & 0 \\ B_{31} & 0 & B_{33} \end{bmatrix} \begin{Bmatrix} A_1 \\ A_2 \\ A_3 \end{Bmatrix} \tag{7}$$

The application of a standard least square procedure to solve Eq. (7) results in an equation of the form

$$\begin{Bmatrix} \bar{w}_1 \\ \bar{w}_2 \\ \bar{w}_3 \end{Bmatrix} = \begin{bmatrix} \bar{B}_{11} & \bar{B}_{12} & \bar{B}_{13} \\ \bar{B}_{21} & \bar{B}_{22} & \bar{B}_{23} \\ \bar{B}_{31} & \bar{B}_{32} & \bar{B}_{33} \end{bmatrix} \begin{Bmatrix} A_1 \\ A_2 \\ A_3 \end{Bmatrix} \tag{8}$$

where $\bar{B}_{12}$, $\bar{B}_{13}$, $\bar{B}_{23}$, $\bar{B}_{32}$ are no longer equal to zero.This means that an uncareful application of a least square procedure can effectively lead to a transfer of information across Mach lines in a manner that is physically impossible in a supersonic flow. It follows therefore that the PCKFM requires the application of a piecewise least-square procedure that avoids violating the supersonic flow rules for transfer of information. Referring to Eq. (7), this can be accomplished by determining A_1 using W_1 and B_{11} (with a least-square procedure). Substitution of the above value of A_1 in the downwash equation relating to box 2 [in Eq. (7)] similarly yields the value of A_2. The value of A_3 is determined in an identical manner. Mathematically, the piecewise least-square procedure yields the following closed form solution for Eq. (7) (presented for illustrative purposes only)

$$\begin{Bmatrix} A_1 \\ A_2 \\ A_3 \end{Bmatrix} = \begin{bmatrix} [B_{11}^T B_{11}]B_{11}^{-1T} & 0 & 0 \\ -[B_{22}^T B_{22}]^{-1} B_{22} B_{21} [B_{11}^T B_{11}]B_{11}^T & [B_{22}^T B_{22}]^{-1} B_{22}^T & 0 \\ -[B_{33}^T B_{33}]^{-1} B_{33} B_{31} [B_{11}^T B_{11}]B_{11}^T & 0 & [B_{33}^T B_{33}]^{-1} B_{33}^T \end{bmatrix} \begin{Bmatrix} w_1 \\ w_2 \\ w_3 \end{Bmatrix}$$

where the superscript T denotes the transpose matrix. The computer program does not assume any closed form solution, and it successively computes A_1, then A_2 and so on, until all pressure polynomial coefficients relating to all boxes are evaluated.

Integration of the Pressure Polynomials

The aerodynamic forces and moments are obtained by integration of the pressure after evaluating the coefficients of the pressure polynomials. This is done in each box by integrating in the chordwise directions first and then integrating in the spanwise direction. The integration in the chordwise direction is performed by a Gaussian type integration which takes the wing boundary pressure singularity into account whenever the particular wing boundary coincides with the boundary of the box. The same procedure is applied when integrating the above chordwise integrands in the spanwise direction of the box. However, in order to maintain the accuracy of this spanwise integration, it should be performed in two stages whenever a box such as box 1 in Fig. 2 happens to exist. In this latter case, the spanwise integration over box 1 should be performed between the root of the wing and point B, again between point B and point C, and then from point C to the tip of the wing. The reason for this three-stage spanwise integration lies in the fact that box 1 (Fig. 2) has a chord discontinuity at points B and C. These discontinuities affect the accuracy of the spanwise integration unless performed as indicated above.

Results

The results presented herein were obtained using an IBM 370-168 computer with programs that employ a double precision accuracy. In many cases the subsonic PCKFM program formed the basis for the new program. In one particular case changes were introduced in the data to avoid changes in the basic program. This relates to the two-stage integration mentioned toward the end of the previous section. To avoid changes in the program, the wing was divided into additional boxes so as to prevent chord discontinuities from lying within the boxes and thus avoid the need for a two-stage spanwise integration of the chordwise integrand. This increase in the number of boxes adversely affects the CPU times cited, but has a negligible adverse effect on the accuracy. This fact is mentioned whenever such results are presented.

Preliminary Results for a Single Box Wing

In the following, preliminary results will be presented with the objective of establishing the numerical values for the different parameters involved in the numerical integration of the kernel-downwash expression. A delta wing in steady supersonic flow is chosen for this purpose, and its aspect ratio AR and the flight Mach number are such that the PCKFM yields a single box which covers the whole wing. The results presented in Tables 1-3 therefore relate to a single box delta wing with $AR=4$ and $M=\sqrt{2}$.

Table 1 shows the influence of varying the spanwise width of the singular region III on the accuracy of the aerodynamic coefficients. The exact linearized aerodynamic coefficients for this wing are obtained using the following well-known expressions for a delta wing (with supersonic LE)

$$C_{L\alpha}=4/\beta \qquad C_{M\alpha}=\frac{-4}{\beta}\left(\frac{2}{3}-x_M\right) \tag{9}$$

where x_M denotes the location of the pitching axis. For the aforementioned delta wing, Eq. (9) yields $C_{L\alpha}=4$ and $C_{M\alpha}=-8/3$ (for $x_M=0$). It can be seen that the percentage errors $\epsilon_{L\alpha}$ and $\epsilon_{M\alpha}$ in the aerodynamic coefficients are within 1% of the exact values. The default value for the size of region III was chosen (in the computer program) to be 0.02 of the wing semispan. Table 2 shows the influence on the aerodynamic coefficients of varying the degree of the spanwise polynomial expansion in region III (for the single-box delta wing mentioned earlier). It can be seen that convergence is very rapid, yielding in all cases errors below 1% (even for first-order polynomial). The default value for the degree of the spanwise polynomial in region III was chosen to be 3, since it produced more accurate results for a wide range of wings which were subsequently tested.

The influence of varying the number of integration points in each spanwise region of integration was investigated. Convergence was found to be very rapid, and three in-

Table 4 Comparison of aerodynamic coefficients with exact values over a range of Mach numbers (delta wing, $\mathcal{R}=2$, $k=0$)[a]

M	Exact linear theory value, C_L	$C_{L\alpha}$	$\epsilon_{L\alpha}$, %	Exact linear theory value, C_M	$C_{M\alpha}$	$\epsilon_{M\alpha}$, %	CPU,s present method
1.1	2.956	2.910	1.6	−1.971	−1.942	1.5	2.52
1.2	2.823	2.782	1.5	−1.882	−1.856	1.4	2.52
1.4	2.608	2.584	0.9	−1.739	−1.723	0.9	2.51
1.6	2.430	2.419	0.5	−1.620	−1.612	0.5	2.45
1.8	2.276	2.274	0.1	−1.517	−1.515	0.1	2.44
2.0	2.141	2.146	0.2	−1.427	−1.429	0.1	2.46
$\sqrt{5}$	2.000	2.009	0.5	−1.333	−1.337	0.3	2.43
2.5	1.746	1.777	1.8	−1.164	−1.184	1.7	5.16

[a]See Table 1, footnotes 2-7.

Table 5 Comparison of aerodynamic coefficients with exact values over a range of Mach numbers (rectangular wing, $\mathcal{R}=2$, $k=0$)[a]

M	Exact linear theory value, C_L	$C_{L\alpha}$	$\epsilon_{L\alpha}$, %	Exact linear theory value, C_M	$C_{M\alpha}$	$\epsilon_{M\alpha}$, %	CPU,s present method
$\sqrt{1.25}$	4.000	3.987	0.3	−1.333	−1.289	3.3	12.46
1.2	3.768	3.765	0.1	−1.500	−1.476	1.6	16.28
$\sqrt{2}$	3.000	3.001	0.0	−1.333	−1.309	1.8	5.52
2	1.976	1.945	1.6	−0.932	−0.915	1.8	6.05

[a]See Table 1, footnotes 2-5, 7,8.

Table 6 Comparison of aerodynamic coefficients with exact values over a range of aspect ratios (delta wing, $M=\sqrt{2}$, $k=0$)[a]

$\mathcal{R}$	Exact linear theory value, C_L	$C_{L\alpha}$	$\epsilon_{L\alpha}$, %	Exact linear theory value, C_M	$C_{M\alpha}$	$\epsilon_{M\alpha}$, %	CPU,s present method
1.0	1.465	1.439	1.8	−0.977	−0.960	1.7	2.50
1.5	2.073	2.045	1.4	−1.382	−1.364	1.3	2.61
2.0	2.594	2.571	0.9	−1.729	−1.714	0.9	2.57
3.0	3.411	3.412	0.0	−2.274	−2.273	0.0	2.53
4.0	4.000	4.023	0.6	−2.667	−2.678	0.4	2.41
5.0	4.000	4.076	1.9	−2.667	−2.715	1.8	4.98
6.0	4.000	4.065	1.6	−2.667	−2.710	1.6	5.00
8.0	4.000	4.061	1.5	−2.667	−2.707	1.5	5.17

[a]See Table 1, footnotes 2-7.

Table 7 Comparison of aerodynamic coefficients with exact values over a range of aspect ratios (rectangular wing, $M=\sqrt{2}$, $k=0$)[a]

$\mathcal{R}$	Exact linear theory value, C_L	$C_{L\alpha}$	$\epsilon_{L\alpha}$, %	Exact linear theory value, $C_{M\alpha}$	$C_{M\alpha}$	$\epsilon_{M\alpha}$, %	CPU,s present method
1.0	2.000	1.989	0.6	−0.677	−0.646	3.1	5.67
2.0	3.000	3.001	0.0	−1.333	−1.308	1.8	6.51
4.0	3.500	3.566	1.9	−1.667	−1.694	1.6	6.06
8.0	3.750	3.844	2.5	−1.833	−1.878	2.5	5.57

[1]See Table 1, footnotes 2-5, 7,8.

Table 8 Comparison of aerodynamic coefficients with exact values (delta wing, $\mathcal{R}=2$, $M=2.5$, $k=2$)[a]

Aerodynamic coefficient	Exact linear theory value		Present method value		ϵ, %
C_{LH}	0.322	(85.8 deg)	0.329	(86.7 deg)	2.2
C_{MH}	2.118	(−94.4 deg)	2.155	(−93.6 deg)	1.7
$C_{L\alpha}$	2.725	(49.9 deg)	2.764	(51.2 deg)	1.4
$C_{M\alpha}$	19.544	(−126.8 deg)	19.821	(−125.5 deg)	1.4

[a]See Table 1, footnotes 2-7, 9.

Table 9 Comparison of aerodynamic coefficients with exact values (rectangular wing, $\mathcal{R}=2$, $M=2$, $k=0.3$)[a]

Aerodynamic coefficient	Exact linear theory value		Present method value		ϵ, %
C_{LH}	0.589	(88.3 deg)	0.569	(88.5 deg)	1.2
C_{MH}	0.277	(−92.1 deg)	0.279	(−91.8 deg)	0.7
$C_{L\alpha}$	1.985	(7.4 deg)	2.009	(7.6 deg)	1.2
$C_{M\alpha}$	0.943	(−169.4 deg)	0.950	(−169.2 deg)	0.7

[a] See Table 1, footnotes 2-5, 7, 8, 10.

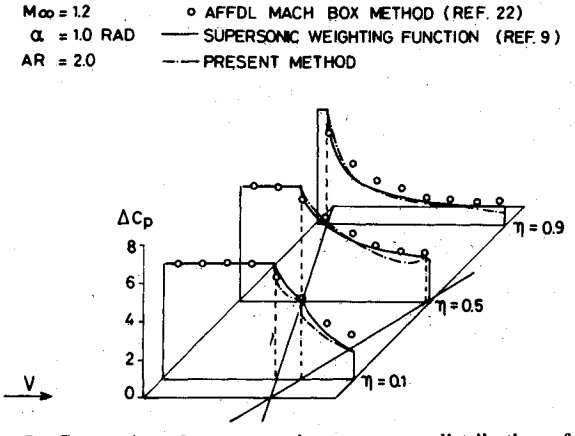

Fig. 5 Comparison between various pressure distributions for a rectangular wing.

tegration points per spanwise integration region were chosen as the default value in the program.

The influence of varying the number of integration points in the chordwise direction was also investigated. The resulting error was within 1% and three chordwise integration points per chordwise integration region were chosen as the default value in the program.

Finally, the effect of varying the number of orthogonal pressure polynomials on the convergence of the aerodynamic coefficients is shown in Table 3. Here again, the whole delta wing represents a single box. It can be seen that the results are more sensitive to the number of spanwise pressure polynomials than to the number of chordwise polynomials. In both directions, three polynomials were chosen (implying quadratic variation over the wing) as default values in the program.

Results for Different Wings

The first group of results relates to delta wings and to rectangular wings over a range of aspect ratios and Mach numbers in steady supersonic flow. Table 4 shows a comparison between the exact linearized results and those obtained by the present method for a delta wing with $\mathcal{R}=2$ over a range of Mach numbers. The exact values for delta wings with supersonic LE are given by Eq. (9). For delta wings with subsonic LE, the aerodynamic coefficients are given by

$$C_{L\alpha}=\frac{\pi}{2}\frac{\mathcal{R}}{E(\bar{m})} \qquad C_{M\alpha}=\frac{\pi}{2}\frac{\mathcal{R}}{E(\bar{m})}\left(\frac{2}{3}-x_M\right) \tag{10}$$

where $E(\bar{m})$ is the complete elliptic integral of the second kind with modulus $\bar{m}=(1-m^2)$ and with $m=\beta\cot\Omega_{LE}$ where Ω_{LE} denotes the LE sweep angle. The errors can be seen to be less than 1.8% in all cases. Table 5 shows a similar comparison over a range of Mach numbers for a rectangular wing with $\mathcal{R}=2$. Here the errors are within 3.3%. The exact linearized values $C_{L\alpha}$ and $C_{M\alpha}$ for rectangular wings were obtained from Ref. 2 and are based on the formulation of Ref. 20. Table 6 shows a comparison between the exact linearized results and those obtained by the present method for delta wings at $M=\sqrt{2}$ over a range of aspect ratios. The errors can be seen to lie within 1.9%. Table 7 shows a similar comparison relating to rectangular wings at $M=\sqrt{2}$. The errors lie within 3.5% in all cases.

Table 10 Comparison of aerodynamic coefficients with exact values (clipped delta wing, $\mathcal{R}=2.22$—see Fig. 3, $M=\sqrt{5}$, $k=0$, with full span flap)[a]

Aerodynamic coefficient	Exact linear theory value	Present method value	ϵ, %
$C_{L\alpha}$	1.917	−1.922	0.3
$C_{L\beta}$	0.844	−0.838	0.8
$C_{H\beta}$	0.114	−0.119	4.4

[a] See Table 1, footnotes 2-7.

It should be mentioned here that the CPU values cited in Tables 4-7 are often higher than those normally required by the present method. The reason lies in an unnecessary artificial increase in the number of boxes allocated on the wing (as already stated earlier). The CPU values should therefore be regarded as being indicative only, with actual values being equal or smaller than the shown values.

Tables 8 and 9 relate to delta wings in unsteady oscillatory pitch and plunge modes. Table 8 shows a comparison between the aerodynamic coefficients obtained by the present method and those obtained by an exact linearized method[21] for a delta wing with $\mathcal{R}=2, M=2.5$, and reduced frequency $k=2$ (based on the root chord). It can be seen that the error in the modulus of the aeordynamic coefficients are within 2.2%, and the errors in phase angle are less than 1.3 deg. Table 9 shows a similar comparison for a rectangular wing with $\mathcal{R}=2$, $M=2, k=0.3$ (based on the root chord). It can been seen that the errors in the modulus are less than 1.2% and the errors in the phase angle are less than 0.3 deg. The exact linearized values appearing in Table 9 were obtained from Ref. 2 based on the formulation of Ref. 20 (valid for $k\leq\beta^2/M_\infty^2$).

Table 10 shows a comparison between exact[22] and computed aerodynamic coefficients for a clipped delta wing (see Fig. 3) with full span flap in steady flow at $M_\infty=\sqrt{5}$. The errors in $C_{L\alpha}$ and $C_{L\beta}$ are within 0.8%. The hinge moment coefficient $C_{H\beta}$ yields an error of 4.4%.

Finally, Fig. 5 shows an illustration of the pressure distribution as obtained by the present method together with a comparison of similar pressure distributions, as obtained by other methods.

Conclusions

The extension of the PCKFM to the supersonic flow regime appears to yield results with high accuracy and with rapid convergence characteristics. The method had been tested in planar configurations only. The next step will involve its extension to nonplanar multi-wing configurations.

Appendix: Location of the Collocation Points

For completeness, the location of the normalized collocation points are given by the following approximate

expressions:

Supersonic LE box ($w[\bar{\xi}]=1$]

$$x_{cj}=\cos\frac{(2j-1)\pi}{2M_p} \qquad j=1,2,\ldots,M_p$$

Subsonic LE box [$w(\bar{\xi})=1/\sqrt{1+\bar{\xi}}$]

$$x_{cj}=-\cos\frac{j\pi}{M_p+1} \qquad j=1,2,\ldots,M_p$$

Intermediate box and supersonic TE box [$w(\bar{\xi})=1$]

$$X_{cI}\approx -0.9$$

$$X_{cj}=-\cos\frac{(j-1)\pi}{M_n} \qquad j=2,3,\ldots,M_n \text{ for } M_n\leq 5$$

Subsonic TE box [$w(\bar{\xi})=\sqrt{1-\bar{\xi}}$]

$$X_{cj}=-\cos\frac{(4j-3)\pi}{4M_n-1} \qquad j=1,2,\ldots,M_n$$

where M_p represents the number of pressure polynomials assumed and $M_n=M_p+1$.

In the spanwise direction the collocation points are determined as follows:

Supersonic LE box, intermediate box and TE box [$W(\bar{\eta})=1$]

$$Y_{cj}=\cos\frac{(2j-1)\pi}{2M_p} \qquad j=1,2,\ldots,M_p$$

Subsonic LE box [$W(\bar{\eta})=1$]

Y_{cj}'s are located at the zeros of the polynomials orthogonal to

$$\sqrt{1-\bar{\eta}} \qquad j=1,2,\ldots,M_p$$

Intermediate box and TE box [$W(\bar{\eta})=\sqrt{1-\bar{\eta}}$]

Y_{cj}'s are located at the zeros of the polynomials orthogonal to

$$1/\sqrt{1-\bar{\eta}} \qquad j=1,2,\ldots,M_n$$

References

[1] Pines, S., Dugundji, J., and Neuringer, J., "Aerodynamic Flutter Derivatives for a Flexible Wing with Supersonic and Subsonic Edges," *Journal of the Aeronautical Sciences,* Vol. 22, Oct. 1955, pp. 693-700.

[2] Donato, V.W. and Huhn, C.R., "Supersonic Unsteady Aerodynamics for Wings with Trailing Edge Control Surfaces and Folded Tips," AFFDL-TR-68-30, Aug. 1968.

[3] Chipman, R.R., "An Improved Mach-Box Approach for the Calculation of Supersonic Oscillatory Pressure Distributions," *Proceedings of the AIAA/ASME/SAE 17th Structures, Structural Dynamics and Materials Conference,* May 1976, pp. 615-625.

[4] Appa, K., "Integrated Potential Formulation of Unsteady Supersonic Aerodynamics for Interacting Wings," AIAA Paper 75-762, May 1975.

[5] Giesing, J.P., "Oscillatory Supersonic Lifting Surface Theory Using Finite-Element Doublet Representation," AIAA Paper 75-761, May 1975.

[6] Burkhart, T.H., "Numerical Application of Evvard's Supersonic Wing Theory to Flutter Analysis," AIAA Paper 80-0741, May 1980.

[7] Evvard, J., "Use of Source Distributions for Evaluating Theoretical Aerodynamics of Thin Finite Wings at Supersonic Speeds," NASA TR 951, June 1949.

[8] Rowe, W.S., Winther, B.A., and Redman, M.C., "Prediction of Unsteady Aerodynamic Loadings Caused by Leading Edge and Trailing Edge Control Surface Motions in Subsonic Compressible Flow-Analysis and Result," NASA CR-2543, Aug. 1975.

[9] Cunningham, A.M., "Oscillatory Supersonic Kernel Function Method for Isolated Wings", *Journal of Aircraft,* Vol. 11, Oct. 1974, pp. 609-615.

[10] Nissim, E. and Lottati, I., "Oscillatory Subsonic Piecewise Continuous Kernel Function Method," National Technical Information Service, Springfield, Va., Paper N77-73109, 1977.

[11] Nissim, E. and Lottati, I., "Oscilatory Subsonic Piecewise Continuous Kernel Function Method," *Journal of Aircraft,* Vol. 14, June 1977, pp. 515-516.

[12] Lottati, I. and Nissim, E., "Three Dimensional Oscillatory Piecewise Continuous Kernel Function Method—Part I: Basic Problems," *Journal of Aircraft,* Vol. 18, May 1981, pp. 346-351.

[13] Lottati, I., and Nissim, E., "Three Dimensional Oscillatory Piecewise Continuous Kernel Function Method—Part II: Geometrically Continuous Wings," *Journal of Aircraft,* Vol. 18, May 1981, pp. 352-355.

[14] Lottati, I. and Nissim, E., "Three Dimensional Oscillatory Piecewise Continuous Kernel Function Method—Part III: Wings with Geometrical Discontinuities," *Journal of Aircraft,* Vol. 18, May 1981, pp. 356-363.

[15] Albano, E. and Rodden, W.P., "A Doublet-Lattice Method for Calculating Lift Distributions on Oscillating Surfaces in Subsonic Flows," *AIAA Journal,* Vol. 7, Feb. 1969, pp. 279-285.

[16] Kalman, T.P., Rodden, W.P., and Giesing, J.P., "Application of the Doublet-Lattice Method to Nonplanar Configurations in Subsonic Flow," *Journal of Aircraft,* Vol. 8, June 1971, pp. 406-413.

[17] Abramowitz, M. and Stegun, I.A., "Handbook of Mathematical Functions," Dover Publication Inc., N.Y., 1965, pp. 771-802, 875-924.

[18] Harder, R.L., and Rodden, W.P., "Kernel Function for Nonplanar Oscillating Surfaces in Supersonic Flow," *Journal of Aircraft,* Vol. 8, Aug. 1971, pp. 677-679.

[19] Desmarais, R.N., "Programs for Computing Abscissas and Weights for Classical and Non-Classical Gaussian Quadrature Formulas," NACA TN-D-7924, Oct. 1975.

[20] Nelson, H.C. Rainey, R.A., and Watkins, C.E., "Lift and Moment Coefficients Expanded to the Seventh Power of Frequency for Oscillatory Rectangular Wings in Supersonic Flow and Applied to a Specific Flutter Problem," NACA TN 3076, April 1954.

[21] Walsh, J., Zartarian, G., and Voss, H.M., "Generalized Aerodynamic Forces on Delta Wings with Supersonic Leading Edges," *Journal of the Aeronautical Sciences,* Vol. 21, Nov. 1954, pp. 739-748.

[22] Ii, J.M., Borland, C.J., and Hogley, J.R., "Prediction of Unsteady Aerodynamic Loadings of Nonplanar Wings and Wing-Tail Configurations in Supersonic Flow, Part I—Theoretical Development, Program Usage and Application," AFFDL-TDR-71-108, March 1972.